Journal of The Electrochemical Society, **156** (2) J28-J31 (2009)
0013-4651/2008/156(2)/J28/4/$23.00 © The Electrochemical Society

Growth and Field Emission of Reactive Sputtered Pd–PdO Core–Shell Nanoflakes on Platinum

Chien-Jung Huang,[a] Fu-Ming Pan,[a,z] Tai-Cheng Tzeng,[a] Li-Chang,[a] and Jeng-Tzong Sheu[b]

[a]*Department of Materials Science and Engineering and* [b]*Institute of Nanotechnology, National Chiao-Tung University, Hsinchu, 30010 Taiwan*

Palladium oxide (PdO) was deposited on platinum by reactive sputter deposition, and the PdO thin film grown on the Pt substrate had a flakelike morphology. The nanosized flake had a core–shell structure with a single Pd grain encapsulated by a crystalline PdO surface layer. The formation of the PdO capped nanoflakes was ascribed to a large interfacial stress due to a lattice mismatch between PdO and Pt. Field emission characteristics of the nanoflakes were studied and a field-enhancement factor of 791 was obtained.
© 2008 The Electrochemical Society. [DOI: 10.1149/1.3035822] All rights reserved.

Manuscript submitted September 30, 2008; revised manuscript received October 24, 2008. Published December 4, 2008.

Palladium oxide (PdO) is a p-type semiconductor with a bandgap of 0.8–2.2 eV.[1-3] It is thermally stable up to ~800°C, at which the oxide decomposes into the metallic Pd state.[2] Because of various particular chemical, optical, and electrical properties, PdO is of great importance in many technological applications, such as catalysis,[4,5] photoelectrolysis,[6] and electron field emission.[7] Nanomaterials usually exhibit distinct material properties from bulks due to a large surface-to-volume ratio and the quantum-confined electronic structure. PdO nanostructures have recently been prepared and investigated for their intriguing properties. For instance, PdO nanofibers have been synthesized by electrospinning using palladium acetate/polycarbonate solutions,[8] and nanotips were produced by relaxing large compressive stresses during thermal oxidation of Pd films.[9] In this study, we used reactive sputter deposition to deposit PdO thin film on the Pt substrate, and found that nanosized flakes with a core–shell structure, in which a Pd grain was encapsulated by a crystalline PdO layer, were produced. Many two-dimensional (2D) nanomaterials, such as nanowalls,[10] nanosheets,[11] and nanoflakes,[12] have been widely studied, such the 2D core–shell nanostructure. The possible growth mechanism of the core–shell nanoflake and field-emission properties of the nanoflakes are discussed in this paper.

Experimental

Deposition of PdO nanoflakes was carried out in a radio-frequency (rf) magnetron sputter deposition system. The palladium target was 2 in. in diameter with a purity of 99.99%. Reactive sputter deposition was performed with a gas mixture of Ar (20 sccm) and O_2 (20 sccm) at the working pressure of 9×10^{-3} Torr and the rf power of 50 W. The sample preparation was started with the thermal growth of a SiO_2 layer 100 nm thick on a 6 in. p-type (100) silicon wafer. A Ti layer 10 nm thick was then deposited by electron-beam evaporation (E-beam) on the oxide as an adhesion layer for the subsequently E-beam deposited Pt thin film with a thickness of 30 nm. The nanoflake film was then deposited on the Pt film at various temperatures. The surface morphology of the PdO nanoflake thin film was examined by scanning electron microscopy (SEM, JEOL JSM-6500F), and the chemical composition was characterized by X-ray photoelectron spectroscopy (XPS) and Auger electron spectroscopy (Thermo VG 350). X-ray diffractometry (XRD, PANalytical X'Pert Pro) and transmission electron microscopy (TEM, JEOL JEM-3000F) were used to study the microstructure of the nanoflakes. Field-emission measurements of the nanoflakes were carried out under a vacuum condition of 5.0×10^{-6} Torr with a high-voltage measurement source (Keithley 237), using the planar capacitor measurement configuration. The separation between the nanoflake cathode and the indium tin oxide coated anode plate was 100 μm.

[z] E-mail: fmpan@faculty.nctu.edu.tw

Results and Discussion

Figures 1a and b show the plane-view SEM images of PdO thin films reactive sputter deposited on the Pt substrate for 15 min at 25 and 200°C, respectively. For both the deposition temperatures, the PdO thin films had a flakelike morphology. The 60°-tilted SEM image of the PdO deposited at 200°C shown in Fig. 1c indicates that the PdO thin film was composed of many individual fish scalelike flakes vertically standing on the substrate. While the length of the nanoflakes increased with the deposition temperature, the heights of the nanoflakes deposited at 25 and 200°C were the same. PdO nanoflakes deposited at 200°C had a width of ~15 to 20 nm, a length of ~250 to 280 nm, and a height of ~200 nm.

The glancing-angle X-ray diffraction spectra of as-deposited nanoflake thin films are shown in Fig. 2. For the nanoflakes grown at 25°C, four reflection peaks, corresponding to the (111), (200), (220), and (311) planes of the Pd face-centered cubic (fcc) structure, were clearly observed, and a small peak situated at 33.8° was identified as the PdO(101) plane. As the growth temperature was raised to 200°C, while the four diffraction peaks for metallic Pd were still

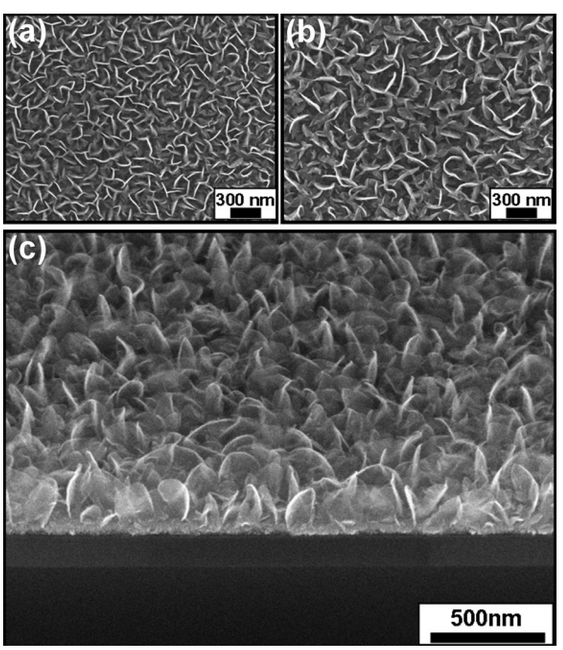

Figure 1. SEM images of Pd–PdO nanoflakes deposited on the Pt substrate at (a) 25 and (b) 200°C. (c) 60°-tilted SEM image for nanoflakes deposited at 200°C.

Downloaded on 2014-04-25 to IP 140.113.38.11 address. Redistribution subject to ECS terms of use (see ecsdl.org/site/terms_use) unless CC License in place (see abstract).

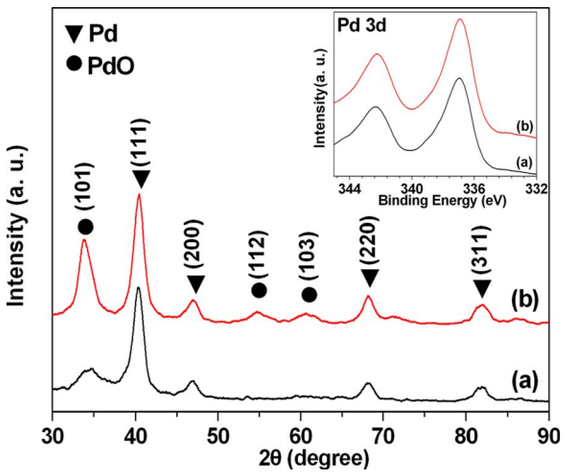

Figure 2. (Color online) XRD spectra of Pd–PdO nanoflakes deposited on the Pt substrate at (a) 25 and (b) 200°C. The inset shows the Pd (3d) XPS spectra of nanoflakes deposited at (a) 25 and (b) 200°C.

detected with similar intensity ratios, the peak intensity of the PdO(101) plane significantly increased and two more peaks due to the PdO(112) and (103) planes became obvious. This result indicated that the deposited nanoflakes were composed of crystalline Pd and PdO, and the PdO phase deposited at 200°C had a better crystallinity than that at 25°C. Also shown in Fig. 2 are two Pd (3d) XPS spectra of nanoflakes deposited separately at 25 and 200°C (inset). For both the two deposition temperatures, the Pd ($3d_{5/2}$) peak situated at ~336.9 eV corresponds to the chemical state of PdO. No signal at 335.0 eV was detected, indicating that metallic Pd was absent on the surface of the nanoflakes. Combined with the XRD results, the XPS analysis suggested that the nanoflake was capped by a PdO surface layer with a thickness probably larger than five times the inelastic mean-free path of the Pd (3d) photoelectrons (~5 nm), and the PdO layer had a strong (101) texturing. A TEM study further showed that a single-crystalline Pd grain was encapsulated by the PdO layer.

The TEM images of a nanoflake deposited at 200°C is shown in Fig. 3. The nanoflake was separated from the thin film by ultrasonic agitation in ethanol. The observation of Moiré fringes in the TEM image of Fig. 3a indicated that different crystalline phases were present in the thin nanoflake. The inset shows the selected area electron diffraction (SAED) pattern of the nanoflake. Two sets of diffraction spots, marked separately by the solid and dashed lines, can be clearly identified from the SAED pattern, revealing that the nanoflake was composed of two single crystalline phases. Because the two diffraction sets have a symmetrical arrangement with respect to each other, the two corresponding-crystals should be epitaxially aligned with each other in the nanoflake. The diffraction set with orientation labels of $(0\bar{2}2)$, $(1\bar{1}1)$, and (200) corresponded to the Pd fcc structure with the zone axis of [011], and the other set with labels of $(1\bar{1}2)$, (101), and (110) was due to the PdO tetragonal structure with the zone axis of $[\bar{1}11]$. The high-resolution TEM (HRTEM) image of an edge area of the nanoflake (highlighted by the circle in Fig. 3a) is shown in Fig. 3b. The fringe spacings of 0.269 and 0.218 nm corresponded to the lattice spacings of PdO(101) and (110), respectively. The fast-Fourier transform diffraction (FFTD) pattern (inset of Fig. 3b) of the area marked by the square in the HRTEM image indicated a single-crystalline phase in the edge area of the nanoflake. The TEM analysis clearly demonstrated that the nanoflake had an epitaxial core–shell structure with a Pd single-crystalline grain surrounded by the PdO surface layer.

To explore the growth mechanism of the Pd–PdO nanoflakes, we have grown nanoflakes for various deposition times. The SEM images of Fig. 4 show variation in surface morphology of the nanoflake thin film deposited at 25°C as a function of the deposition time. The thin film deposited for 2 min had a very smooth surface (Fig. 4a). Islands began to emerge on the film surface after 3 min deposition, and a few islands already exhibited a flakelike feature (Fig. 4b). The flakes grew larger both in length and height with increasing the deposition time, as shown by Fig. 4c and d. The observation implied that the nanoflakes were not directly formed on the substrate via the Volmer–Weber growth mode, but rather evolved due to a certain driving force developing in the early stage of the film deposition. The XPS spectrum of the smooth thin film deposited for 2 min is shown in Fig. 5. A close examination of the Pd (3d) peaks indicated that, within the probe depth of the XPS measurement, PdO was the only chemical state of Pd. Because Pt (4f) photoelectrons from the substrate were also detected, the presence of metallic Pd in the thin film could be ruled out. Thus, the XPS analysis suggested that PdO was the primitive product at the beginning of the reactive sputter deposition, and very likely the precursor for the formation of the crystalline Pd grain in the nanoflake.

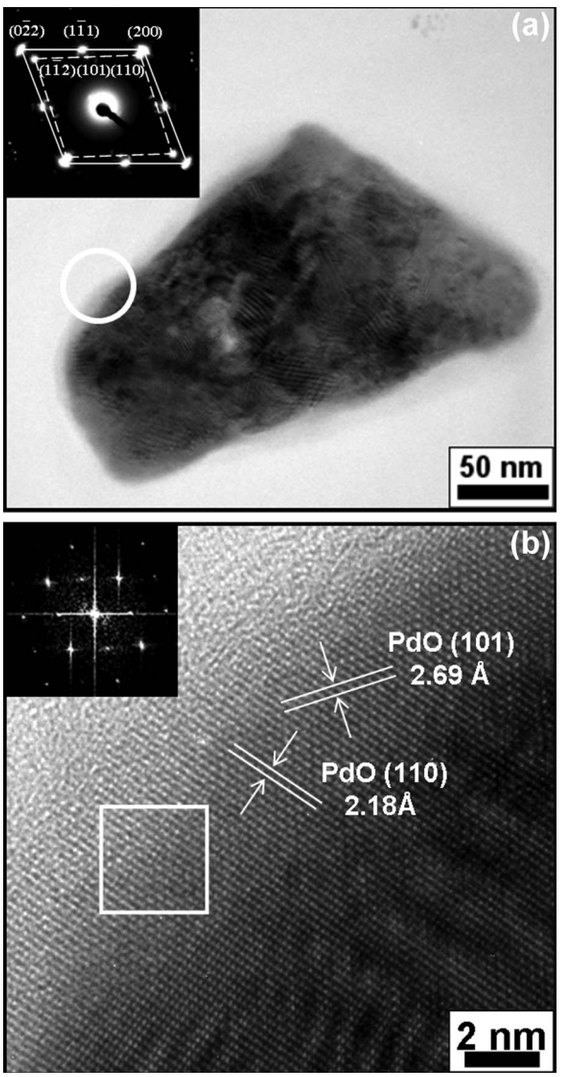

Figure 3. (a) TEM image of a Pd–PdO nanoflake separated from the nanoflake thin film deposited at 200°C for 15 min. The inset is the SAED pattern of the nanoflake. Two diffraction sets are identified to correspond to the Pd fcc structure (solid line) and the PdO tetragonal structure (dashed line). (b) The HRTEM image of the edge area marked by circle in (a). The inset shows the FFTD pattern of the area marked by square in (b).

Downloaded on 2014-04-25 to IP 140.113.38.11 address. Redistribution subject to ECS terms of use (see ecsdl.org/site/terms_use) unless CC License in place (see abstract).

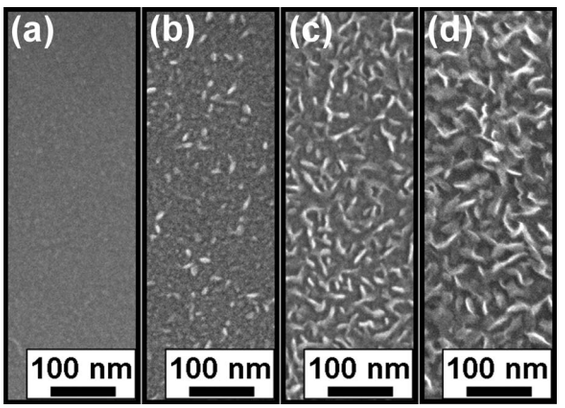

Figure 4. SEM images of Pd–PdO nanoflakes deposited on the Pt substrate at 25°C for (a) 2, (b) 3, (c) 4, and (d) 5 min.

To study the role of the Pt substrate in the growth of the Pd–PdO core–shell nanoflakes, we have also reactive sputter deposited PdO at 200°C on a sputter-deposited Ti and a thermally grown SiO_2 thin film for comparison. Nanoflakes with a geometric shape like that shown in Fig. 1 were also produced on both the thin-film substrates. According to XRD and XPS analyses, PdO was the only chemical composition of the nanoflakes deposited on the Ti and SiO_2 substrates. In addition, TEM analysis showed that the PdO nanoflake was a single-crystalline grain (not shown). Based on simple surface energy consideration, formation of the crystalline PdO nanoflake rather than a spherical structure suggested that the growth of the PdO nanoflake was via an anisotropic process. The anisotropic growth process might be related to the planar coordination arrangement of Pd and oxygen atoms in the PdO crystal lattice, in which each Pd atom is coordinated with four oxygen atoms. Because the nanoflake grown on the SiO_2 and Ti surfaces was composed of only the crystalline PdO phase, the Pt surface must play a critical role in the formation of Pd–PdO core–shell nanoflakes on the Pt substrate. The observation that the core–shell nanoflake grown on the Pt substrate has the same geometric shape as the crystalline PdO nanoflake grown on the SiO_2 and Ti substrates seemed to suggest that PdO was first deposited on the Pt substrate, followed by formation of the crystalline Pd core sheet with a shape compliant with that of the PdO nanoflake. This suggestion is in agreement with the discussion about Fig. 4 and 5.

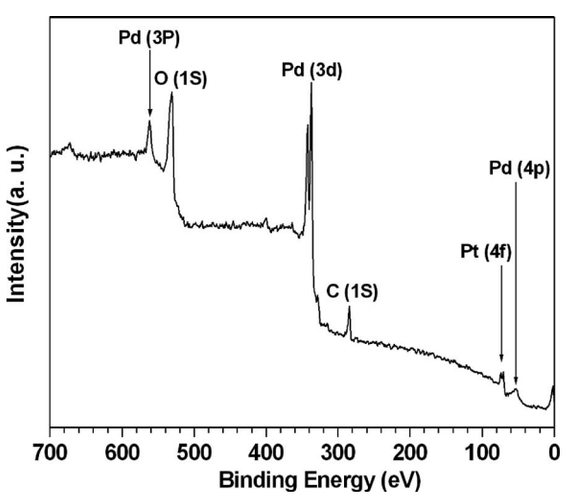

Figure 5. XPS survey spectra for 2 min deposition at a substrate temperature of 25°C.

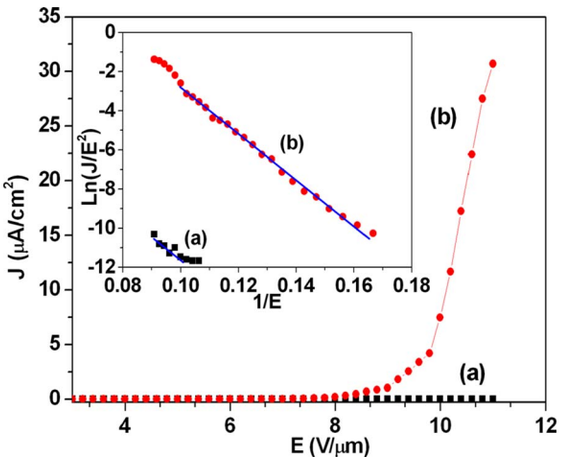

Figure 6. (Color online) Field-emission *J-E* curves of Pd–PdO nanoflakes deposited on the Pt substrate at (a) 25 and (b) 200°C. The corresponding FN plots of the *J-E* curves (a) and (b) are shown in the inset.

PdO has a crystal structure of tetragonal cooperite structure with the lattice constants $a = b = 3.0434$ Å and $c = 5.3363$ Å.[13] The Pt fcc structure has lattice constants $a = b = c = 3.924$ Å, which are very close to the lattice constants of the Pd fcc structure ($a = b = c = 3.891$ Å). As the PdO film grew thicker, the interfacial stress between the PdO deposit and the Pt substrate became so large, due to the large lattice mismatch, that decomposition of the PdO phase and lattice reconstruction could be initiated at the interface. Furthermore, the negligible difference in the lattice parameters between the Pd and Pt lattices (0.8%) could facilitate nucleation of the Pd crystal on the Pt substrate during the initial stage of the phase transformation. The lattice mismatch between the PdO and Pd lattices was very large as well; thereby, a large interfacial stress always existed at the PdO–Pd interface. Therefore, the phase transformation from PdO into Pd must progressively proceed at the interface between the growing Pd crystal and the PdO surface layer, which was continuously deposited on the nanoflake during the reactive sputter deposition. The continuous stress building up between the Pd core sheet and the PdO surface layer would limit the thickness of the PdO layer deposited on the nanoflake. According to the XPS and HRTEM analyses, the PdO surface layer was probably ~4 to 6 nm in thickness. Because the thickness of the nanoflake was ~15 to 20 nm as discussed above, the Pd core sheet in the nanoflake must be just a few nanometers in thickness. From the SAED diffraction pattern shown in Fig. 3a, the PdO surface layer was epitaxially aligned with the Pd crystal. It has been previously reported that the PdO(110) plane was epitaxially aligned with the Pd(200) plane when Pd particles supported on SiO_2 were oxidized in oxygen.[14] The same epitaxial arrangement was also observed in this study. The lattice spacing of the PdO(110) and the Pd(200) planes are 2.11 and 1.95 Å, respectively. Compared with other lattice planes of the two crystal structures, these two planes have the smallest difference in the lattice spacing, and are more likely to be epitaxially arranged with each other. Within this thickness range of the PdO surface layer, the epitaxial arrangement of the Pd–PdO core–shell structure seemed to be relatively stable.

PdO is a semiconductor and, therefore, not an ideal field-emission material in respect to its relatively high electrical resistivity. However, the metallic Pd core sheet can increase the conductivity of the Pd–PdO core–shell nanoflake as a whole, and thereby may improve the field-emission efficiency. Moreover, because the nanoflakes vertically standing on the substrate had a sharp top edge and a high aspect ratio in terms of the thickness and height, they are expected to have good field-emission properties. Figure 6 shows the field-emission current density–applied field (*J-E*) curves of the PdO

Downloaded on 2014-04-25 to IP 140.113.38.11 address. Redistribution subject to ECS terms of use (see ecsdl.org/site/terms_use) unless CC License in place (see abstract).

nanoflakes deposited for 15 min at 25 and 200°C. According to the *J-E* curve, nanoflakes deposited at 200°C had a much better field-emission performance than that deposited at 25°C. At the applied field of 11 V μm^{-1}, nanoflakes deposited at 200 and 25°C had a field-emission current density of 30.7 $\mu A\ cm^{-2}$ and 4 $nA\ cm^{-2}$, respectively. The linear Fowler–Nordheim (FN) plots shown in the inset of Fig. 6 indicated that the field emission followed the FN field-emission mechanism. The turn-on field of the nanoflakes deposited at 25 and 200°C was determined to be 10 and 6 V μm^{-1}, respectively. The turn-on field was herein defined as the field at the intersection of the two straight lines extrapolated separately from the linear rising segment and the background of the FN plot. The better field-emission characteristics of the nanoflake deposited at 200°C may be attributed to that the PdO surface layer on the nanoflake deposited at 200°C had a well-textured and better crystalline structure than that deposited at 25°C. According to the FN theory,[15] the field enhancement factor (β), which is strongly dependent on the geometric structure of the field emitter, can be approximated by

$$\beta = -\frac{B\phi^{3/2}}{S} \quad [1]$$

where $B = 6.83 \times 10^3$ ($V\ eV^{-3/2}\ \mu m^{-1}$), ϕ is the work function of the emitter, and S is the slope of the FN plot. The FN plot slope of the nanoflake deposited at 200°C was −108.3. The β values of the nanoflake were thus determined to be 791, assuming a work function of 5.4 eV for PdO.[16] The β value of Pd–PdO nanoflakes is comparable to that of Co_3O_4 nanowalls[17] and some previously reported one-dimensional nanoemitters, such as carbon nanotubes and Si nanotips.[18,19] Due to the desirable field-emission characteristics, combined with an easy preparation method and chemical and thermal stabilities, the Pd–PdO nanoflakes can be considered as a potential emitter for field-emission applications.

Conclusion

In summary, we have deposited PdO on the Pt substrate by reactive sputter deposition. At temperatures 200°C and below, the PdO thin film grown on the Pt substrate had a flakelike morphology. TEM, XRD, and XPS studies revealed that the nanoflake had a core–shell structure with a single Pd grain encapsulated by a crystalline PdO surface layer. The PdO layer was about 4–6 nm in thickness and epitaxially aligned with the Pd lattice. Formation of the Pd–PdO nanoflakes resulted from the large interfacial stress due to the large lattice mismatch between the PdO surface layer and the Pt substrate. The Pd grain growth in the nanoflake was facilitated by the close similarity in the lattice parameters of the Pt and Pd fcc crystal structures. Because of the sharp top edge and a high aspect ratio, the Pd–PdO nanoflake exhibited a field emission efficiency comparable to many one-dimensional nanoemitters. A β value of 791 was obtained for the nanoflake deposited at 200°C.

Acknowledgments

This work was supported by the National Science Council of Taiwan under contract no. NSC96-2221-E009-109-MY3. Technical support from National Nano Device Laboratories is gratefully acknowledged.

National Chiao Tung University assisted in meeting the publication costs of this article.

References

1. E. A. Sales, G. Bugli, A. Ensuque, M. J. Mendes, and F. Bozon-Verduraz, *Phys. Chem. Chem. Phys.*, **1**, 491 (1999).
2. T. Arai, T. Shima, T. Nakano, and J. Tominaga, *Thin Solid Films*, **515**, 4774 (2007).
3. J. R. McBride, K. C. Hass, and W. H. Weber, *Phys. Rev. B*, **44**, 5016 (1991).
4. P. Gélin and M. Primet, *Appl. Catal., B*, **39**, 1 (2002).
5. L. V. Nosova, M. V. Stenin, Y. N. Nogin, and Y. A. Ryndin, *Appl. Surf. Sci.*, **55**, 43 (1992).
6. M. P. Dare-Edwards, J. B. Goodenough, A. Hamnett, and A. Katty, *Mater. Res. Bull.*, **19**, 435 (1984).
7. E. Yamaguchi, K. Sakai, I. Nomura, T. Ono, M. Yamanobe, N. Abe, and T. Hara, *J. Soc. Inf. Disp.*, **5**, 345 (1997).
8. P. Viswanathamurthia, N. Bhattarai, H. Y. Kim, D. I. Cha, and D. R. Lee, *Mater. Lett.*, **58**, 3368 (2004).
9. S. Aggarwal, A. P. Monga, S. R. Perusse, R. Ramesh, V. Ballarotto, E. D. Williams, B. R. Chalamala, Y. Wei, and R. H. Reuss, *Science*, **287**, 2235 (2000).
10. S. W. Kim, S. Fujita, M. S. Yi, and D. H. Yoon, *Appl. Phys. Lett.*, **88**, 253114 (2006).
11. Y. C. Yhu and Y. Bando, *Chem. Phys. Lett.*, **372**, 640 (2003).
12. N. G. Shang, F. C. K. Au, X. M. Meng, C. S. Lee, I. Bello, and S. T. Lee, *Chem. Phys. Lett.*, **358**, 187 (2002).
13. D. B. Rogers, R. D. Shannon, and J. L. Gillson, *J. Solid State Chem.*, **3**, 314 (1971).
14. S. Penner, B. Jenewein, H. Gabasch, B. Klötzer, D. Wang, A. Knop-Gericke, R. Schlögl, and K. Hayek, *J. Chem. Phys.*, **125**, 094703 (2006).
15. R. H. Fowler, L. W. Nordheim, *Proc. R. Soc. London, Ser. A*, **119**, 173 (1928).
16. J. Rogal, K. Reuter, and M. Scheffler, *Phys. Rev. B*, **69**, 075421 (2004).
17. T. Yu, Y. Zhu, X. Xu, Z. Shen, P. Chen, C. T. Lim, J. T. Thong, and C. H. Sow, *Adv. Mater. (Weinheim, Ger.)*, **17**, 1595 (2005).
18. R. C. Smith, D. C. Cox, and S. R. P. Silva, *Appl. Phys. Lett.*, **87**, 103112 (2005).
19. T. M. Chen, F. M. Pan, J. Y. Hung, S. C. Wu, C. F. Chen, and L. Chang, *J. Electrochem. Soc.*, **154**, D215 (2007).

Downloaded on 2014-04-25 to IP 140.113.38.11 address. Redistribution subject to ECS terms of use (see ecsdl.org/site/terms_use) unless CC License in place (see abstract).